

Partitioning of Free Energy Gain between the Photoisomerized Retinal and the Protein in Bacteriorhodopsin[†]

Andrei K. Dioumaev,[‡] Leonid S. Brown,[‡] Richard Needleman,[§] and Janos K. Lanyi^{*‡}

Department of Physiology & Biophysics, University of California, Irvine, California 92697, and Department of Biochemistry, Wayne State University, Detroit, Michigan 48201

Received April 24, 1998; Revised Manuscript Received May 28, 1998

ABSTRACT: Photoisomerization of the *all-trans*-retinal of bacteriorhodopsin to 13-*cis*,15-*anti* initiates a sequence of thermal reactions in which relaxation of the polyene chain back to *all-trans* is coupled to various changes in the protein and the translocation of a proton across the membrane. We investigated the nature of this high-energy state in a genetically modified bacteriorhodopsin. When the electric charges of residues 85 and 96, the two aspartic acids critical for proton transport, are both changed to what they become after photoexcitation of the wild-type protein, i.e., neutral and anionic, respectively, the retinal assumes a thermally stable 13-*cis*,15-*anti* configuration. Thus, we have reversed cause and effect in the photocycle. It follows that when the 13-*cis*,15-*anti* isomeric state is produced by illumination, in the wild type it is unstable initially only because of conflicts with the retinal binding pocket. Later in the photocycle, the free energy gain is transferred from the chromophore to the protein. Before recovery of the initial state, it will come to be represented entirely by the free energy of the changed protonation states of aspartic acids 85 and 96.

Excess free energy in transmembrane ion pumps, signal receptors, and enzymes is often generated at a location different from where it is utilized for the transport, conformation change, or catalysis. How is ΔG stored in these proteins? In bacteriorhodopsin, the light-driven proton pump, the free energy gain is from absorption of a photon by the *all-trans*,15-*anti*-retinal chromophore (1–5). Photoisomerization to 13-*cis*,15-*anti* is followed by proton transfer from the retinal Schiff base to Asp-85 (M intermediate), release of a proton from a complex of hydrogen-bonded residues and water (6–9) to the extracellular surface, a large-scale protein conformation change (10) that lowers the pK_a of Asp-96, reprotonation of the Schiff base from Asp-96 (N intermediate), and reprotonation of Asp-96 from the cytoplasmic surface (11). Reisomerization of the retinal (O intermediate) and deprotonation of Asp-85 recover the initial state (12–15). The free energy gain is initially in the redistribution of electrons and bond rotations and/or twists in the polyene chain of the retinal, and in charge separation between the Schiff base and its counterion. As in other pumps, it is not clear at what time in the reaction cycle this excess energy is passed to the protein and in what form, so as to allow transport and the creation of a transmembrane proton potential.

We searched for ways to modify the protein so it would resemble one of the photocycle intermediates, with the idea

that if the appropriate changes are introduced they might, without illumination, cause the retinal to assume the otherwise unstable 13-*cis*,15-*anti* configuration. In such an intermediate of the photocycle, the excess free energy will be stored no longer in the retinal but in the protein. A clue that this reversal of cause and effect in the photocycle might be possible was the finding that in the unilluminated D85N mutant three species resembling photocycle intermediates exist in a pH-dependent equilibrium (16). The yellow species with unprotonated Schiff base has a changed overall protein structure similar to the M intermediate of the wild type (17, 18). The other two, purple and blue,¹ resemble the N and O intermediates, respectively, at least in their absorption spectra in the visible. Another clue was that at pH <3, where Asp-85 is protonated, solid-state NMR spectra of samples labeled with ¹³C at C₁₂ and C₁₄ of the retinal revealed (19) the existence of four species, instead of the expected binary mixture of 13-*cis*,15-*syn* and *all-trans*,15-*anti* in dark-adapted bacteriorhodopsin (20). The additional species could be 13-*cis*,15-*anti* and *all-trans*,15-*syn* (19). The possibility of a stable 13-*cis*,15-*anti* configuration was surprising, because unlike the 13-*cis*,15-*syn* polyene chain (which is linear like *all-trans*,15-*anti* and exists in thermal equilibrium with it), the 13-*cis*,15-*anti*-retinal is strongly bent. It is unstable, and therefore a high-energy configuration. One would assume that the reason is a conflict of the polyene chain and the positively charged Schiff base, steric and electrostatic, respectively, with the retinal binding pocket (21, 22).

[†]This work was funded partly by grants from the National Institutes of Health (GM 29498 to J.K.L.), the Department of Energy (DEFG03-86ER13525 to J.K.L.), and the U. S. Army Research Office (DAAL03-92-G-0406 to R.N.).

* Correspondence should be addressed to this author. E-mail: jlanyi@Orion.oac.uci.edu.

[‡] University of California.

[§] Wayne State University.

¹ In the case of the wild-type protein, the designations “blue” and “purple” have referred to the pigment with protonated and anionic Asp-85, respectively. In the D85N mutant, however, residue 85 is permanently uncharged, and the blue to purple color shift has a different origin.

MATERIALS AND METHODS

Strains. The D85N, D85N/F42C, and D85N/D96N bacteriorhodopsin mutants were constructed and expressed in *Halobacterium salinarum* as described before (17). Purple membranes containing these mutant proteins were prepared by a standard method (23).

Spectroscopy in the Visible. Changes in absorbance were measured at selected wavelengths after pH jump produced with rapid mixing (≤ 2.5 ms) in a HiTech Model SF-61 stopped-flow assembly, using a single-beam kinetic spectrometer (7, 8). Where pulse photoexcitation was used, it was provided as a 7 ns flash, at 532 nm, from a frequency-doubled Continuum Surelite I Nd:YAG laser. All measurements were done at 20 °C.

Infrared and Raman Spectroscopy. Fourier transform infrared spectra were measured either as difference spectra after laser excitation with a Bruker IFS66/S spectrometer in the step-scan mode as described before (9, 24) or as absolute spectra in an Attenuated Total Reflection cell (25). In the latter case, the spectra at various pHs were compared after normalizing the amplitudes of their amide II bands. FT-Raman spectra were measured in a Bruker IFS66/S-FRA106/S spectrometer with 1064 nm Raman excitation, as previously described (24). As in the visible, all infrared measurements were at 20 °C.

RESULTS AND DISCUSSION

We examined the isomeric configuration of the retinal in the D85N/F42C mutant, where the equilibrium of the blue and purple species¹ is at a pH lower than the pK_a of the Schiff base. Thus, interference from deprotonation of the Schiff base (yellow species) is less than in D85N. If the dissociation of Asp-96 is the cause of the blue-to-purple transition, the purple species will contain not only the uncharged Asn-85 but also an anionic Asp-96. As far as the charges of these residues, this species would then resemble the N photointermediate, in which Asp-85 is protonated but Asp-96 is not (15, 26). The questions are as follows: Is Asp-96 indeed anionic in the purple species, and is the configuration of the retinal affected by residues 85 and 96?

pH-Dependent Shift of the Absorption Maximum. We found that the chromophore of D85N/F42C, like that of D85N (16, 17), changes from blue (absorption maximum at 595 nm) to purple (absorption maximum at 573 nm), but with an apparent pK_a of about 8. Figure 1a,b shows that raising the pH rapidly from 6 to 8 converts the blue chromophore to purple with a time constant of 33 ms. This result rules out the possibility that the purple species is a photoproduct of the blue at the higher pH, despite all efforts to exclude light from the samples. Deprotonation of the Schiff base is less extensive and much slower (seconds) than the blue-to-purple shift. The absorption changes, that describe the photochemical reactions of the chromophore, also distinguish the purple from the blue species. As Figure 1c shows, the photocycle of the purple species is quite different from that of the blue, and dominated by red-shifted intermediates, similarly to the photoreaction of the 13-*cis*-, 15-*syn* isomer (27, 28), and the 13-*cis*-, 15-*anti* in the N intermediate (29–31), in wild-type bacteriorhodopsin. The absorption change upon photoexcitation was tested with a laser flash 300 ms after the shift to pH 8. The result (Figure

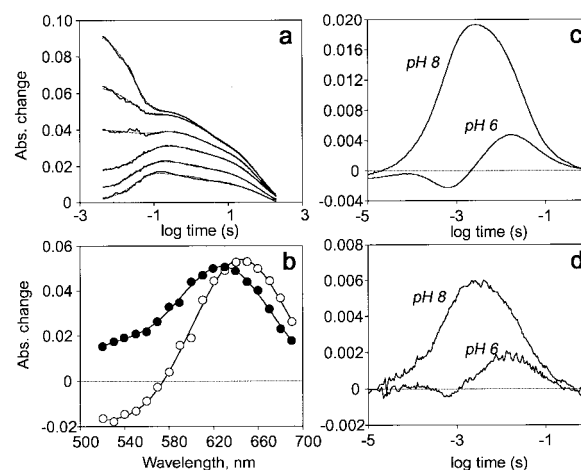


FIGURE 1: Spectral changes from the blue-to-purple transition in D85N/F42C bacteriorhodopsin, and changed photoreaction, after a pH jump. The pH was shifted from 6.0 to 8.0, and either the absorption of D85N/F42C bacteriorhodopsin (250 mM NaCl, 50 mM Bis-tris-propane) was monitored at various wavelengths, or the absorption change applied 300 ms after mixing was followed. (a) Absorption changes at 520, 540, 560, 580, 600, and 620 nm, in order of increasing amplitudes, after the pH jump (solid lines). The kinetics are described by three exponentials (the two slowest were seen in D85N/D96N also (24) (dashed lines). (b) Amplitude spectra for the first kinetic component ($\tau = 33$ ms, open circles) and the other two combined ($\tau > 2$ s, filled circles). The most rapid component represents the blue-to-purple transition of the chromophore. The slower changes correspond to deprotonation of the Schiff base. (c) Absorption change at 640 nm after flash excitation at pH 6.0 and 8.0. The purple and blue species exhibit different photoreactions. (d) Absorption change at 640 nm upon flash excitation 300 ms after shift of the pH from 6.0 to 8.0. In the control experiment, the pH remained at 6.0. The traces shown are differences between those with and without flash. The detection of changed photoreaction as early as 300 ms justifies the conclusion that it originates from the purple species.

1d) verified that the purple species arises early after the pH jump, consistent with the time constant of the change of the maximum of the chromophore absorption band, and not from other possible species that might form more slowly.

Photocycle of the D85N/F42C Mutant. The photochemical reactions of the purple species are illustrated in Figure 2 with infrared difference spectra measured at various times after flash photoexcitation. As in the photocycle of D85N (17, 32), the Schiff base does not deprotonate significantly. Otherwise, the spectra contain novel features. Of the labeled bands in Figure 2, the one at 1743 cm^{-1} refers to protonation of Asp-96, the pair at 1668 and 1647 cm^{-1} to a shift of the amide I band, the pair at 1552 and 1510 cm^{-1} to a shift of the ethylenic stretch band, those at 1394 and 1306 cm^{-1} to coupled N–H and C_{15} –H in-plane bending, and those at 1184 and 1167 cm^{-1} to C–C stretch bands from 13-*cis*/*all-trans* isomerization. Thus, the spectra indicate the photoisomerization of predominantly 13-*cis*-retinal to *all-trans*, a prominent shift of the amide I band to higher frequency, and protonation of what must be initially unprotonated Asp-96, i.e., changes that are in the reverse direction from the well-described photocycle of the wild type (12–15). The difference spectra between the photoproduct and the purple species in Figure 2 are in fact virtually identical to the spectrum of bacteriorhodopsin minus the N intermediate (15). It appears that in this photocycle an N-like initial species is converted to a transient state that is like unphotolyzed bacteriorhodopsin.

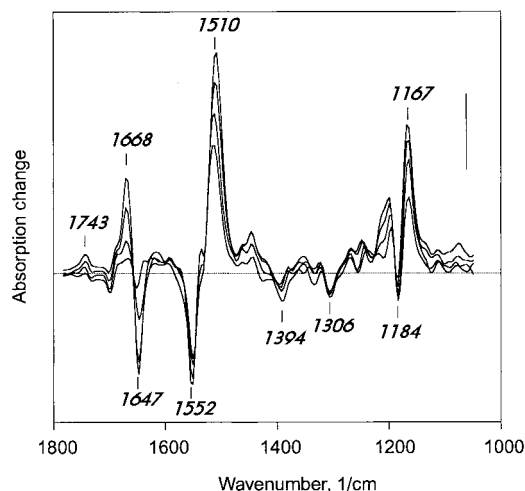


FIGURE 2: Fourier transform infrared difference spectra of the purple species of D85N/F42C bacteriorhodopsin after flash photoexcitation. The spectra shown were measured at 5 μ s, 60 μ s, 300 μ s, and 1.3 ms, in order of increasing amplitudes, after photoexcitation with a laser pulse. The bar corresponds to an optical density change of 4×10^{-4} . The bands seen (as discussed in the text) are the major bands also in the difference spectrum between the N intermediate and wild-type bacteriorhodopsin, exhibiting similar relative amplitudes but inverted signs (15, 37).

Titration of Asp-96 in Various Mutants. The pK_a of Asp-96 in the wild type is above 11 (25), but was predicted to be lower in Asp-85 mutants (17, 18). The difference spectra in Figure 2 that indicate protonation of Asp-96 after photoisomerization of the purple species of D85N/F42C, and the fact that in D85N/D96N the purple species does not form at any pH (24), suggested that the difference between the purple and the blue could be that in the former Asp-96 is dissociated. This was confirmed directly by infrared titration of the C=O stretch band of the protonated Asp-96, as before (25) at 1740 cm^{-1} . From spectroscopic titrations in the visible region, the conversion between the blue and purple species occurs with a pK_a of 9.3 ± 0.3 in D85N (16) and 7.8 ± 0.3 in D85N/F42C. The pH dependence of the amplitude of the 1740 cm^{-1} band revealed a pK_a of 9.4 ± 0.3 in D85N and 8.2 ± 0.3 in D85N/F42C (not shown), in good agreement with the values from the visible. As expected, D85N/D96N exhibited no C=O band with significantly pH-dependent amplitude up to pH 11. In D85N/F42C (as in D85N), therefore, Asp-96 is protonated in the blue species and anionic in the purple. The pK_a of Asp-96 is apparently lowered through a protein conformation change when Asp-85 loses its charge (17, 18), and becomes further lowered by the additional F42C mutation because replacement of Phe-42 that flanks the aspartic acid (33) with a more polar residue decreases the hydrophobicity of this region.

Identification of the Isomeric Configuration of Retinal in D85N/F42C. Fourier transform Raman spectra are resonance-enhanced (34), and thus originate nearly entirely from the chromophore. Because the Raman excitation is with near-infrared light, the amplitudes of bands from species with unprotonated Schiff base are greatly attenuated. Characteristic vibrational bands, and their shifts in D_2O that reveal isotope effects of the modes coupled to vibrations of the N-H/D bond, will identify the configuration of the $C_{13}=C_{14}$ bond as *cis* or *trans*, and the $C_{15}=N$ bond as *syn* or *anti*. Figures 3 and 4 compare the Raman spectra of the blue and

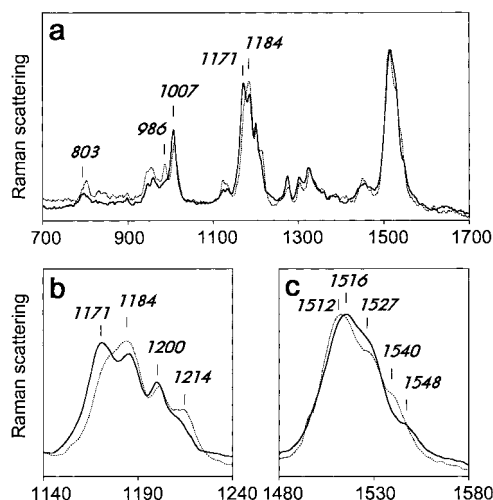


FIGURE 3: Isomeric configuration of retinal in the blue species of D85N/F42C bacteriorhodopsin, from Fourier transform Raman spectra in H_2O and D_2O , measured at a pH or pD ($=pH + 0.4$) of 6.6. Spectra in H_2O are shown with solid lines, those in D_2O with dashed lines. The entire frequency region is shown in (a), the expanded fingerprint and the ethylenic stretch regions in (b) and (c), respectively. As explained in the text, these spectra reveal that the blue species of D85N/F42C is a mixture of *all-trans*, 15-*anti* and 13-*cis*, 15-*syn*, as in dark-adapted wild-type bacteriorhodopsin.

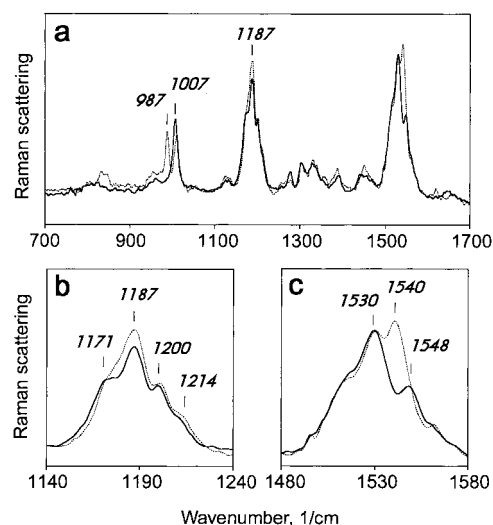


FIGURE 4: Isomeric configuration of retinal in the purple species of D85N/F42C bacteriorhodopsin, from Fourier transform Raman spectra in H_2O and D_2O . The spectra were measured as in Figure 3, but at pH or pD 9.0. Spectra in H_2O are shown with solid lines, those in D_2O with dashed lines. The entire frequency region is shown in (a), the expanded fingerprint and the ethylenic stretch regions in (b) and (c), respectively. Significant differences from the blue species in Figure 3 are seen. These spectra reveal that in the thermally stable purple species of D85N/F42C the retinal is largely 13-*cis*, 15-*anti*, as only in the transient intermediates of the photocycle when the bacteriorhodopsin is wild type.

purple species of D85N/F42C, respectively, each measured in H_2O and D_2O . The blue species consists of a mixture of *all-trans*, 15-*anti* and 13-*cis*, 15-*syn* isomers, as dark-adapted wild-type bacteriorhodopsin (5, 20). The comparable heights of the 1171 and 1184 cm^{-1} C-C stretch bands, and those of the 1516 and 1527 cm^{-1} ethylenic stretch bands, indicate (5, 35, 36) that the retinal is a mixture of *all-trans* and 13-*cis*. The prominent $C_{14}-H$ out-of-plane (HOOP) band at 803 cm^{-1} argues for a 13-*cis*, 15-*syn* configuration (36, 37). The spectrum in D_2O contains the band for N-D rock at

986 cm^{-1} , as expected (5). In Figure 3b, the shift of the $\text{C}_{14}\text{--C}_{15}$ stretch band from 1171 to 1214 cm^{-1} in D_2O confirms that the $\text{C}=\text{N}$ bond is 15-*syn* in the 13-*cis* species (5). The shift of the low-amplitude 1548 cm^{-1} band to 1540 cm^{-1} in D_2O indicates the presence of a small amount of purple species (cf. Figure 4).

In contrast, the purple species contains nearly entirely 13-*cis*,15-*anti*-retinal. This is indicated by the split ethylenic stretch band, the absence of a $\text{C}_{14}\text{--H}$ out-of-plane band despite the 13-*cis* configuration, the lack of the deuterium shift of the $\text{C}_{14}\text{--C}_{15}$ stretch band seen in authentic 13-*cis*,15-*syn* (5) and in the blue species (Figure 3), and the downshift and amplitude increase of the higher frequency ethylenic stretch band in D_2O . The large amplitude of the 1187 cm^{-1} band relative to the one at 1171 cm^{-1} (Figure 4b) indicates that the $\text{C}_{13}\text{--C}_{14}$ bond is mostly *cis*. Absence of the 803 cm^{-1} HOOP band suggests that this 13-*cis* configuration is 15-*anti* rather than 15-*syn*. This is confirmed by lack of the shift of the $\text{C}_{14}\text{--C}_{15}$ stretch band from 1171 to 1214 cm^{-1} in D_2O (Figure 4b), expected for 13-*cis*,15-*syn* (5) and seen in the blue species (Figure 3). In the N intermediate with 13-*cis*,15-*anti*-retinal, this shift is calculated (22) to be only ca. 5 cm^{-1} , consistent with the changes observed. The ethylenic stretch band is split into a pair of bands at 1530 and 1548 cm^{-1} , even though the spectrum in the visible does not reveal the heterogeneity expected if they were from a mixture (not shown). The appearance of the 1530 and 1548 cm^{-1} bands, with the amplitude ratio much as in Figure 4c, is characteristic, however, of the N photointermediate of the wild type (22) in which the retinal is 13-*cis*,15-*anti*. In the N state, the higher frequency band shifts to a 6 cm^{-1} lower frequency and increases in amplitude in D_2O (22), similarly to Figure 4c. Remarkably, Figure 4 demonstrates that the vibrational spectrum of the retinal in the purple species of D85N/F42C is nearly the same as in the N intermediate of the wild-type photocycle (22).

The results we report here indicate that the photoisomerized 13-*cis*,15-*anti*-retinal of bacteriorhodopsin is not an inherently high-energy configuration. Free energy gained upon photoexcitation is stored in the chromophore only as long as the changes of the protein lag behind the changes in the retinal. Once the N intermediate of the photocycle is formed, the charge states of Asp-85 and Asp-96 (residues that change their protonation states in the transport process) fully determine the configuration of the retinal. In this intermediate, the excess free energy acquired during photoisomerization will have passed already from the retinal to the protein. When residue 85 becomes neutral and residue 96 anionic in the wild-type photocycle, the backbone conformation change evident from the shifted amide I band occurs spontaneously, and the retinal binding pocket now accommodates the photoisomerized retinal. Part of the excess free energy of the absorbed photon will have been conserved in the transmembrane gradient of protons when a proton was released to the extracellular surface earlier in the cycle. Nevertheless, the N intermediate is still a high-energy state because a proton is yet to be taken up from the cytoplasmic side, and the recovery of the initial state at the end of the photocycle occurs with a large negative ΔG , being a strongly unidirectional reaction (38). It appears now that the residual free energy at this stage is equivalent to the free energy difference inherent in the changed Coulombic inter-

actions of the two acidic residues most intimately involved in the transport.

REFERENCES

- Mathies, R. A., Lin, S. W., Ames, J. B., and Pollard, W. T. (1991) *Annu. Rev. Biophys. Biophys. Chem.* 20, 491–518.
- Ebrey, T. G. (1993) in *Thermodynamics of membranes, receptors and channels* (Jackson, M., Ed.) pp 353–387, CRC Press, New York.
- Lanyi, J. K. (1993) *Biochim. Biophys. Acta* 1183, 241–261.
- Lanyi, J. K. (1997) *J. Biol. Chem.* 272, 31209–31212.
- Smith, S. O., Myers, A. B., Pardo, J. A., Winkel, C., Mulder, P. P. J., Lugtenburg, J., and Mathies, R. A. (1984) *Proc. Natl. Acad. Sci. U.S.A.* 81, 2055–2059.
- Balashov, S. P., Imasheva, E. S., Govindjee, R., and Ebrey, T. G. (1996) *Biophys. J.* 70, 473–481.
- Brown, L. S., Sasaki, J., Kandori, H., Maeda, A., Needleman, R., and Lanyi, J. K. (1995) *J. Biol. Chem.* 270, 27122–27126.
- Richter, H. T., Brown, L. S., Needleman, R., and Lanyi, J. K. (1996) *Biochemistry* 35, 4054–4062.
- Dioumaev, A. K., Richter, H. T., Brown, L. S., Tanio, M., Tuzi, S., Saitô, H., Kimura, Y., Needleman, R., and Lanyi, J. K. (1998) *Biochemistry* 37, 2496–1506.
- Subramaniam, S., Gerstein, M., Oesterhelt, D., and Henderson, R. (1993) *EMBO J.* 12, 1–8.
- Otto, H., Marti, T., Holz, M., Mogi, T., Lindau, M., Khorana, H. G., and Heyn, M. P. (1989) *Proc. Natl. Acad. Sci. U.S.A.* 86, 9228–9232.
- Braiman, M. S., Mogi, T., Marti, T., Stern, L. J., Khorana, H. G., and Rothschild, K. J. (1988) *Biochemistry* 27, 8516–8520.
- Souvignier, G., and Gerwert, K. (1992) *Biophys. J.* 63, 1393–1405.
- Richter, H. T., Needleman, R., Kandori, H., Maeda, A., and Lanyi, J. K. (1996) *Biochemistry* 35, 15461–15466.
- Zscherp, C., and Heberle, J. (1997) *J. Phys. Chem. B* 101, 10542–10547.
- Turner, G. J., Miercke, L. J. W., Thorgeirsson, T. E., Kliger, D. S., Betlach, M. C., and Stroud, R. M. (1993) *Biochemistry* 32, 1332–1337.
- Kataoka, M., Kamikubo, H., Tokunaga, F., Brown, L. S., Yamazaki, Y., Maeda, A., Sheves, M., Needleman, R., and Lanyi, J. K. (1994) *J. Mol. Biol.* 243, 621–638.
- Brown, L. S., Kamikubo, H., Zimányi, L., Kataoka, M., Tokunaga, F., Verdegem, P., Lugtenburg, J., and Lanyi, J. K. (1997) *Proc. Natl. Acad. Sci. U.S.A.* 94, 5040–5044.
- De Groot, H. J. M., Smith, S. O., Courtin, J., Van den Berg, E., Winkel, C., Lugtenburg, J., Griffin, R. G., and Herzfeld, J. (1990) *Biochemistry* 29, 6873–6883.
- Harbison, G. S., Smith, S. O., Pardo, J. A., Winkel, C., Lugtenburg, J., Herzfeld, J., Mathies, R. A., and Griffin, R. G. (1984) *Proc. Natl. Acad. Sci. U.S.A.* 81, 1706–1709.
- Schulten, K., and Tavan, P. (1978) *Nature* 272, 85–86.
- Fodor, S. P., Ames, J. B., Gebhard, R., van der Berg, E. M., Stoeckenius, W., Lugtenburg, J., and Mathies, R. A. (1988) *Biochemistry* 27, 7097–7101.
- Oesterhelt, D., and Stoeckenius, W. (1974) *Methods Enzymol.* 31, 667–678.
- Brown, L. S., Dioumaev, A. K., Needleman, R., and Lanyi, J. K. (1998) *Biochemistry* 37, 3982–3993.
- Száz, S., Oesterhelt, D., and Ormos, P. (1994) *Biophys. J.* 67, 1706–1712.
- Sasaki, J., Lanyi, J. K., Needleman, R., Yoshizawa, T., and Maeda, A. (1994) *Biochemistry* 33, 3178–3184.
- Hofrichter, J., Henry, E. R., and Lozier, R. H. (1989) *Biophys. J.* 56, 693–706.
- Logunov, I., Humphrey, W., Schulten, K., and Sheves, M. (1995) *Biophys. J.* 68, 1270–1282.
- Yamamoto, N., Naramoto, S., and Ohtani, H. (1992) *FEBS Lett.* 314, 345–347.
- Balashov, S. P. (1995) *Isr. J. Chem.* 35, 415–428.

31. Brown, L. S., Zimányi, L., Ottolenghi, M., Needleman, R., and Lanyi, J. K. (1993) *Biochemistry* 32, 7679–7685.
32. Maeda, A., Sasaki, J., Yamazaki, Y., Needleman, R., and Lanyi, J. K. (1994) *Biochemistry* 33, 1713–1717.
33. Grigorieff, N., Ceska, T. A., Downing, K. H., Baldwin, J. M., and Henderson, R. (1996) *J. Mol. Biol.* 259, 393–421.
34. Sawatzki, J., Fischer, R., Scheer, H., and Siebert, F. (1990) *Proc. Natl. Acad. Sci. U.S.A.* 87, 5903–5906.
35. Smith, S. O., Pardo, J. A., Lugtenburg, J., and Mathies, R. A. (1987) *J. Phys. Chem.* 91, 804–819.
36. Braiman, M. S., and Mathies, R. A. (1980) *Biochemistry* 19, 5421–5428.
37. Maeda, A. (1995) *Isr. J. Chem.* 35, 387–400.
38. Váró, G., and Lanyi, J. K. (1991) *Biochemistry* 30, 5016–5022.

BI980934O